biosensors

MDPI

Review

A Review of Electroactive Nanomaterials in the Detection of Nitrogen-Containing Organic Compounds and Future Applications

Mohanraj Jagannathan [1], Durgalakshmi Dhinasekaran [2], Ajay Rakkesh Rajendran [3] and Sungbo Cho [1,4,*]

[1] Department of Electronic Engineering, Gachon University, Seongnam-si 13210, Republic of Korea; mohanrajpsix@gmail.com or w0han6aj@gachon.ac.kr
[2] Department of Medical Physics, College of Engineering Campus, Anna University, Chennai 600 025, Tamil Nadu, India; durgalakshmi@annauniv.edu or durgaklakshmi@gmail.com
[3] Functional Nano-Materials (FuN) Laboratory, Department of Physics and Nanotechnology, Faculty of Engineering and Technology, SRM Institute of Science and Technology, Kattankulathur 603 203, Tamil Nadu, India; ajayr1@srmist.edu.in or ajayrakkesh@gmail.com
[4] Gachon Advanced Institute for Health Science & Technology, Gachon University, Incheon 21999, Republic of Korea
* Correspondence: sbcho@gachon.ac.kr; Tel.: +82-(31)-750-5321

Abstract: Electrochemical and impedimetric detection of nitrogen-containing organic compounds (NOCs) in blood, urine, sweat, and saliva is widely used in clinical diagnosis. NOC detection is used to identify illnesses such as chronic kidney disease (CKD), end-stage renal disease (ESRD), cardiovascular complications, diabetes, cancer, and others. In recent years, nanomaterials have shown significant potential in the detection of NOCs using electrochemical and impedimetric sensors. This potential is due to the higher surface area, porous nature, and functional groups of nanomaterials, which can aid in improving the sensing performance with inexpensive, direct, and quick-time processing methods. In this review, we discuss nanomaterials, such as metal oxides, graphene nanostructures, and their nanocomposites, for the detection of NOCs. Notably, researchers have considered nanocomposite-based devices, such as a field effect transistor (FET) and printed electrodes, for the detection of NOCs. In this review, we emphasize the significant importance of electrochemical and impedimetric methods in the detection of NOCs, which typically show higher sensitivity and selectivity. So, these methods will open a new way to make embeddable electrodes for point-of-detection (POD) devices. These devices could be used in the next generation of non-invasive analysis for biomedical and clinical applications. This review also summarizes recent state-of-the-art technology for the development of sensors for on-site monitoring and disease diagnosis at an earlier stage.

Keywords: nanomaterials; electrochemical; impedimetric; nitrogen–containing organic compounds; sensors

Citation: Jagannathan, M.; Dhinasekaran, D.; Rajendran, A.R.; Cho, S. A Review of Electroactive Nanomaterials in the Detection of Nitrogen-Containing Organic Compounds and Future Applications. *Biosensors* **2023**, *13*, 989. https://doi.org/10.3390/bios13110989

Received: 11 September 2023
Revised: 3 November 2023
Accepted: 16 November 2023
Published: 18 November 2023

1. Overview of Urea Analysis in Ancient Eras

Over 6000 years ago, diagnostics were first used as an element of laboratory practice. Urine is an inexpensive source for finding nitrogen-containing organic compounds (NOCs) and demonstrates their potential correlation with various illnesses. This excretory biofluid was a primary diagnostic tool in ancient eras and was considered a "divine fluid" by physicians. Babylonian and Egyptian medicos coined the word "uroscopy", which was derived from the Greek "ouron" (i.e., denoting "urine") and "skopeo" (i.e., denoting "examine or inspect"). In 100 B.C., Sanskrit and Hindu cultures classified urine into twenty distinct types based on its color, and it was further named by its sweet taste in a special case called diabetes mellitus [1]. In the 4th century B.C. (460–365), Hippocrates found the presence of filtrates, such as blood, phlegm, and yellow and black bile, in urine [2]. The

predominant theory of Hippocrates' ideas were further redefined precisely by Galen (AD 129–200), followed by a redefinition in the Middle Ages (AD 500–1500), whereby uroscopy played a vital role in all the stages of disease identification [3–5]. Then, in the Renaissance period (AD 1450–1600), uroscopy was developed as a household self-diagnostic tool for monitoring health conditions. Nevertheless, ancient techniques of diagnosis with urine are not practiced nowadays, yet urine remains an effective tool for the early detection of diseases in the modern world [4]. Figure 1 shows the historical evidence related to the conceptualization, differentiation, and development of nanomaterials for the detection of nitrogen-containing organic compounds.

Figure 1. Historical evidence related to the conceptualization, differentiation, and development of nanomaterials for the detection of nitrogen-containing organic compounds.

2. Introduction

In recent decades, the sustainable economic progress of public health has been dependent on the advancement of science and technology. Therefore, the scientific community has predicted the necessities for the development of effective ideal materials, methodologies, and technology transfers. Despite this, researchers are facing many challenges in treating various illnesses (i.e., cancer, diabetes, neurological dysfunction and/or disorder, etc.), managing food safety and quality, and environmental remediation. Typically, nitrogen-containing organic compounds (NOC) (i.e., urea, uric acid, and creatinine) are naturally found in biofluids such as blood, urine, saliva, and sweat [6]. These NOCs are effectively filtered through the kidneys and liver while also being discreetly filtered through the biodegradation of food as well as environmental systems [7]. In addition, the determination of NOCs is an important biomarker for clinical diagnosis and socio-environmental monitoring [8]. Particularly in clinical diagnosis, urine and blood are considered precious tools for identifying liver and kidney function, urinary tract obstruction, heart failure, catabolism of proteins, and even shock and stress [9]. Tables 1 and 2 show the normal NOC levels of urea, uric acid, and creatinine in biofluid. Increasing or decreasing NOC levels can cause various illnesses. Therefore, extensive research on NOCs poses great challenges in terms of precise determination via analytical methods, even in the presence of complex metabolites at a lower concentration. Of these, an enormous number of conventional methods are being used to identify NOCs, including solid-phase extraction (SPE), ultraviolet-visible (UV-visible) spectroscopy, infrared (IR) spectroscopy, flow injection, chromatography techniques coupled with mass spectrometry, fluorimetry, and surface plasmon resonance (SPR) techniques [10–13]. Furthermore, these methods necessitate sophisticated instrumentation, trained individuals, a time-consuming process, pre-sample preparation, etc. Despite this, electrochemical/electroanalytic techniques have shown promise for direct and indirect quantitative and qualitative determination of NOCs, with good sensitivity, selectivity, a rapid response, and feasible economic viability [14,15]. This is due to the fact that biochemical events are converted into electrical signals through the electrochemical biosensor, which is a typical sensing device. Generally, electrochemical techniques have been recognized based on their operational conditions, such as amperometry (i–t), differential pulse voltammetry (DPV), linear pulse voltammetry (LSV), square wave voltammetry (SWV), the current-potential (I–V), and electrochemical impedimetric spectroscopy (EIS). Of these, the EIS method is a quick, non-destructive technique that has recently been used to determine NOCs. Briefly, the EIS involves applying an alternating current at various frequencies to the sample, followed by measuring the impedance response from the sample as a function of frequency. Rather than conventional techniques, the affordable technique of voltametric measurement has been used to determine the redox potential, whereas the potentiometric method is employed to measure precision, selectivity, and sensitivity. Figure 2 depicts the Scopus index bar chart on the number of research publications based on NOC biomarker detection from the period from 2017 to 2022 and towards the future innovation and sustainable development of wearable devices.

Table 1. The normal NOC levels of urea and uric acid in biofluids [16–20].

S. No.	NOC	Age (Years)	Normal Level (Male) (mg dL^{-1})	Age (Years)	Normal Level (Female) (mg dL^{-1})
1	Urea	1–17	7–20	1–17	7–20
		>18	8–24	>18	6–21

Table 1. *Cont.*

S. No.	NOC	Age (Years)	Normal Level (Male) (mg dL^{-1})	Age (Years)	Normal Level (Female) (mg dL^{-1})
2	Uric Acid	1–10	2.4–5.4	1	2.1–4.9
		11	2.7–5.9	2	2.1–5.0
		12	3.1–6.4	3	2.2–5.1
		13	3.4–6.9	4	2.3–5.2
		14	2.7–7.4	5	2.3–5.3
		15	4.0–7.8	6	2.3–5.4
		>16	3.7–8.0	7–8	2.3–55
				9–10	2.3–5.7
				11	2.3–5.8
				12	2.3–5.9
				>13	2.7–6.1

Table 2. The normal NOC level of creatinine in biofluids [21,22].

S. No.	NOC	Age (Years)	Normal Level (Male)	Age (Years)	Normal Level (Female)
1	Serum creatinine	19–75	0.74–1.35 mg dL^{-1}	19–75	0.59–1.04 mg dL^{-1}
	Typical range based on BSA *	19–75	77–160 mL/min/BSA	18–29	78–161 mL/min/BSA
				30–39	72–154 mL/min/BSA
				40–49	67–146 mL/min/BSA
				50–59	62–139 mL/min/BSA
				60–72	56–131 mL/min/BSA
2	Albumin/ creatinine ratio #	19–75	<17 mg/g	19–75	<25 mg/g

* BSA—Body surface area, # Increase in the ratio above this level could be a sign of kidney disease.

Electrochemical methods are used to determine NOC levels in serum, blood, sweat, and urine, and are of great interest to researchers due to their rapid accessibility. In principle, it is necessary to detect NOC levels via either enzymatic or non-enzymatic electrochemical methods. Furthermore, the enzymatic electroanalytical technique is an indirect method that uses enzymes (i.e., urease), which is referred to as an "enzymatic electrochemical sensor", and vice versa for the non-enzymatic method. These enzymatic or non-enzymatic electroanalytical sensors have certain inevitable drawbacks, as follows: immobilization of enzymes; expensive enzyme; incompetent reproducibility; and limited concentration, temperature, pH, and humidity conditions [10,23–28]. On the other hand, development of biomedical devices for rapid, sensitive, and specific detection of biomarker species has been facilitated by the emerging field of nanomaterials and nanofabrication technology. Indeed, the construction and development of integrated nanosensors for the simultaneous detection of a variety of target analytes will remain a major task on the frontier of nanotechnology [29]. Therefore, the state-of-the-art technology in the manufacture of nano-based devices pays great attention to real-time applications, especially in on-site health monitoring products. The characteristics of mesostructured or composite/hybrid nanostructures are distinctly different from those of conventional bulk materials. Usually, the surfaces of a nanoengineered smart material would have been changed to include functionalities that

create binding sites for biomolecules [30]. Then, these nanomaterials were found to have many uses, especially in the development of direct or indirect electrochemical biosensing devices, which are used to measure NOCs at ultra-low concentrations using very small volumes of different clinical samples (i.e., biofluids). Furthermore, the qualitative and quantitative estimation of NOCs has gained immense importance as it offers early diagnosis of several diseases like renal insufficiency, hyperpyrexia, hyperthyroidism, leukemia, diarrheal diseases, diabetes mellitus, and so on [22,31,32]. So, in this review, we have summarized the recent advances in NOC biomarker detection methods through direct or indirect electrochemical and impedimetric-based sensing methods. A wide range of metal oxide nanoparticles and two-dimensional (2D) materials and their nanocomposites have seen considerable progress in their preparation, processing, characterization, and potential applications (Figure 3). In addition, nanofabrication of devices like FETs and printed electronics has resulted in improvements in their performance. Consequently, it is possible to introduce new opportunities in the development of nanoscale devices and make them economically scalable for next-generation sensors, not only biosensors but also sensors in food and environmental monitoring.

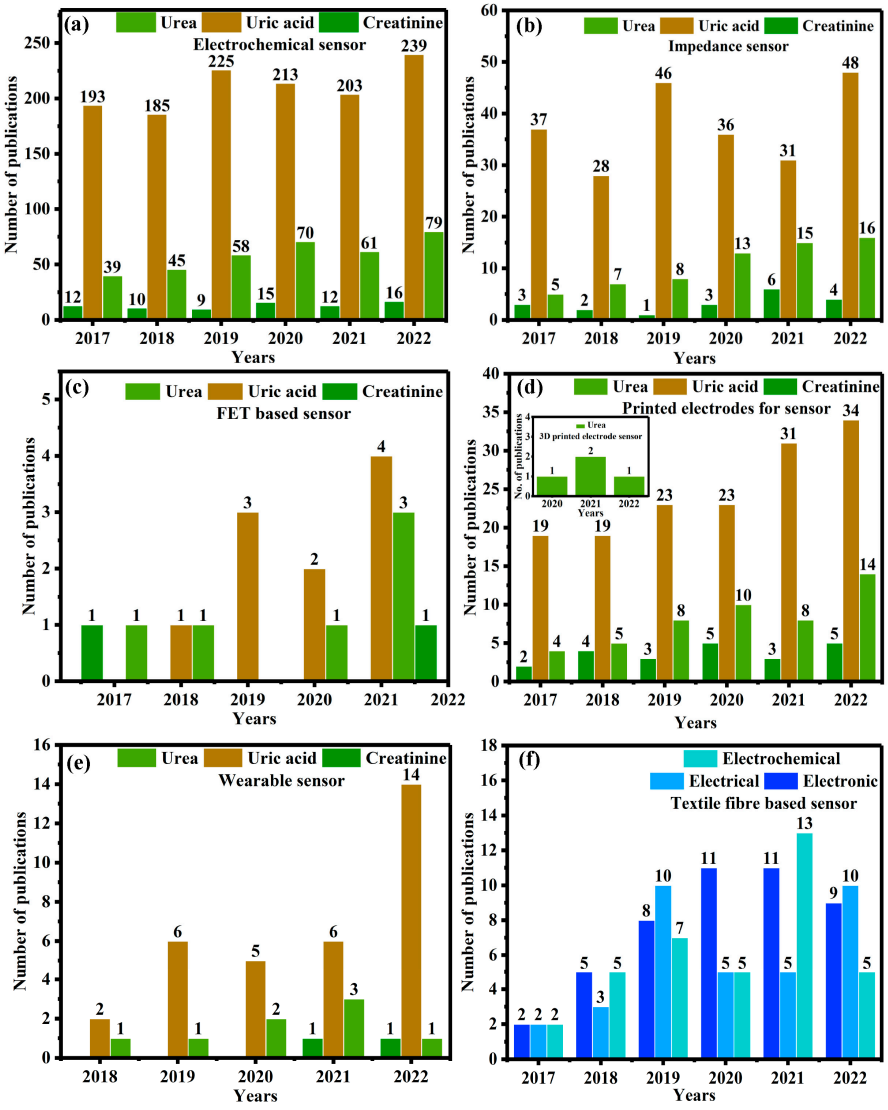

Figure 2. The Scopus index bar chart is related to the number of publications on the topics of (**a**) electrochemical sensors, (**b**) impedimetric sensors, (**c**) FET-based sensors, (**d**) printed electrode sensors, (**e**) wearable sensors, and (**f**) textile fiber-based sensors.

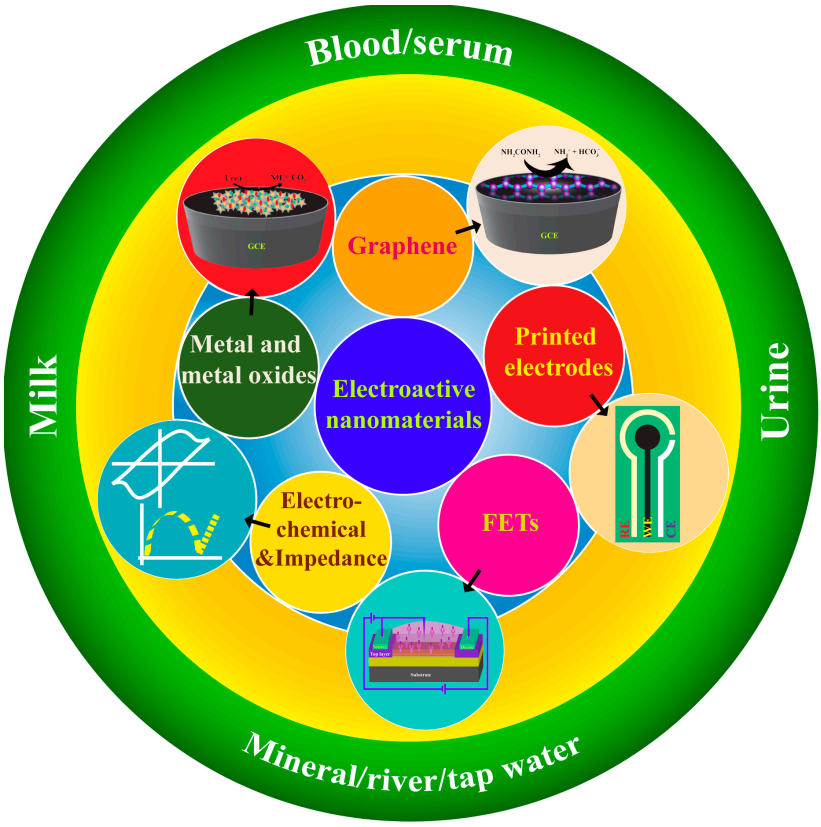

Figure 3. A schematic of the diverse range of NOC sensors that use nanomaterials and their fabricated devices.

3. Nanomaterial-Based Electrochemical Biosensors

Electrochemical biosensors, with their advantages of affordability, and rapid processing and construction, have been extensively used in clinical diagnosis, environmental monitoring, pharmaceutical analysis, and onsite detection of home care products [33]. Integration of electrochemical measurements like amperometry, cyclic voltammetry, electrochemiluminescence, impedimetric, and photoelectrochemistry with recognition units, shows significant advantages during the measurement [34]. These electroanalytical techniques have vast applications, including the determination of excretory metabolites [35], metal ions [36], protein biomarkers [37], DNA [38], neurological disorders [39], etc. However, there are still challenges in quantifying low-quantity biomarkers accurately in a complex system, as it requires precise measurement techniques and material fabrication technology. To overcome these limitations, several functional nanomaterials have been developed in recent decades. Additionally, these nanomaterials can be used as electrocatalysts and can therefore amplify the signal by precise changes upon their measurement [40,41]. However, there is an immediate need for the advancement of nanocatalysts with high performance for the construction and development of next-generation non-invasive electrochemical biosensors.

3.1. Nickel and Its Nanocomposites for NOC Sensing

Transition metal oxides have been extensively used to develop enzymatic/non-enzymatic electrochemical sensors. Metal oxides are highly stable in the ambient atmosphere as well as in an alkaline medium, and the synthesis of metal-based nitride, carbides, and phosphides requires highly sophisticated instruments [42,43]. Therefore, transition metal oxides are more favorable for enzymatic/non-enzymatic electrochemical and impedimetric detection of NOC. At the nanoscale, the properties of metal oxides may be quite different from those of bulk metal oxides. This is because nanoscale metal oxides have a larger

surface area, a small size, and an ordered crystalline structure. In addition, the nanoscale metal oxides can also have hierarchical nanostructures, which could improve the ability of these metal oxides to act as electrocatalysts [44]. Furthermore, the transition metal-based oxides could favor several oxidative states as they enable the detection of target analytes via surface functionalization [45]. Among the numerous metal oxides, nickel nanoparticles and their composites have received great attention for NOC detection. Also, introducing a functional group onto their surfaces further enhances their the molecular-level recognition and/or interaction. Hence, these oxides and their composites possess features such as easy fabrication; controllable shape and size; biocompatibility; catalytic, optical, and electrical properties; strong absorption and stability; and outstanding electron-transfer kinetics [46,47]. With these characteristic features, any electroactive nanomaterial can be used in energy conversion and storage, catalysis, drug delivery systems, and especially chemical and biological sensors [48]. In Figure 4a, nickel-based metal oxides are shown to have good stability, low cost, less toxicity, and good electrical conductivity, as they lead to immobilization, rapid transduction, and signal amplification. Also, the high isoelectric point (i.e., IEP: 9 to 11) of nickel-based metal oxide possesses the ability to enhance the physical adsorption of biomolecules on these metal oxides through electrostatic interactions [49]. Recently, L. Zheng et al. successfully used a method of electroless deposition for the synthesis of Ni-P nanostructures on a paper substrate, which was used for the detection of urea. Here, paper substrates facilitated the highest surface area for electroless deposition of Ni-P nanoflowers, resulting in high electrocatalytic activity for urea detection (Figure 5a–d). A real sample of swimming pool water was used to determine the urea level in this study. Notably, this device has a broad linear range (0 to 1 mM) with a low detection limit (12 μM), higher sensitivity (683.46 μA mM^{-1} cm^{-2}), and quick response time (3 s) [50]. In an alkaline medium, R. H. Tammam and M. M. Saleh studied identical NiOx electrodeposited on a glassy carbon electrode (GCE), which showed better urea oxidation. Further, the corresponding EIS (electrochemical impedimetric spectroscopy) equivalent circuit of the material with a Nyquist plot showed semicircle fitting because of its higher electrocatalytic rates with diffusion-controlled irreversible processes, leading to a lower charge transfer rate [51]. Electrocatalysts like nickel microwire-intercalated cobalt zeolitic imidazole framework (Co-ZIF) without enzymes can be used for the rapid detection of urea. The one-pot solvothermal method was used to make Co-ZIF-nickel nanowires, and the GCE surface was modified with the drop casting method. Arul et al. found that the electrocatalytic oxidation of urea was carried out in the presence of different electrolytes and the composite modified GCE. However, the reaction was more catalytic in Tris-HCl (pH 8.0) buffer solutions than in KOH, acetate, and phosphate buffer solutions, and the way the reaction happened showed that it was controlled by diffusion. Therefore, these authors showed the determination of urea in real samples and the determination was cross validated via the enzymatic method [52]. NiO immobilized on carbonized eggshell (NiO/c-ESM) has also been shown to be a promising material for electrochemically detecting urea in an environmentally friendly way. Lu, S. et al. made a NiO/c-ESM modified with GCE which was used for the electrocatalytic oxidation and reduction of urea in a KOH medium with a significant linear range and limit of detection. CV and square wave voltammetry have were in this study, and it is clear that the oxidation and reduction follow a typical diffusion-controlled process. This process is evident because the NiO/c-ESM system exposes more active sites, which makes it easier for reactants and products to determine urea [53]. Goda, M. A. et al. have also shown that electrochemical deposition can be used to make CuOx-NiOx nanocatalysts with polyaniline/GCE surfaces. So, the NiOx/CuOx/PANI/GCE modified electrode showed better and more stable electrocatalytic performance than the NiOx/CuOx/GCE electrode, as well as easy electron transfer kinetics for urea oxidation [54]. A low-temperature growth method is used for the synthesis of $NiCo_2O_4$ nanoneedles towards the development of enzyme-less detection of urea. Amin, S. et al. proposed non-enzymatic detection of urea in the presence of an alkaline medium and observed that both Ni^{2+} and CO^{2+} oxidized into Ni^{3+} and CO^{3+} after the adsorption

of OH^- ions. Thereafter, urea is adsorbed onto the NiOOH via Ni-O and O-C coordinate linkages, subsequently leading to the direct oxidation of urea, which can take place on the NiOOH and cause the reduced form of $Ni(OH)_2$. Also, the cobalt ions couldn't significantly favor the oxidation of urea, which is due to the presence of $Co^{4+/}Co^{3+}$ active sites [55]. In another work, Tomy, A. M., demonstrated nickel hydroxide nanosheets, which were prepared by the facile co-precipitation method and dropped onto the GCE (Figure 5e,f). The possible sensing mechanism of this electrode exhibited that the amine group in uric acid can bond with the hydroxyl group in the sensor molecule, resulting in the possibility of electron transfer and oxidation of UA to allantol [56]. A detailed comparison of the literature related to NOC sensors using metal oxides is given in Table 3.

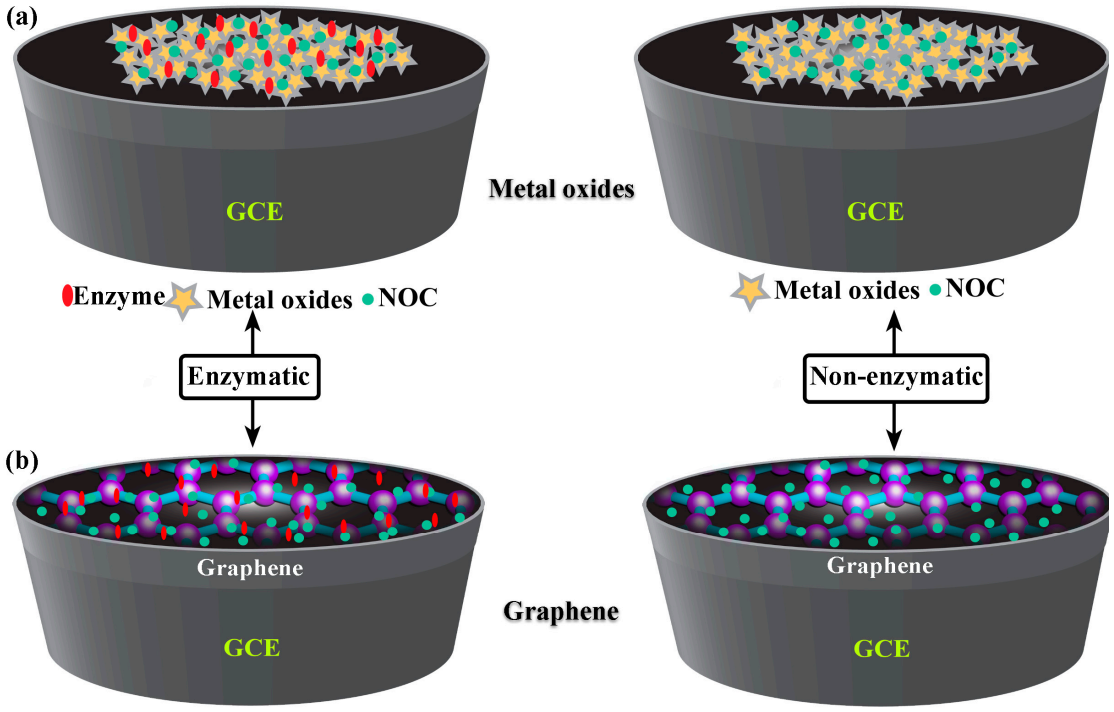

Figure 4. Schematic illustration of the development of (**a**) metal oxides and (**b**) two-dimensional nanomaterials on GCE for the detection of NOCs with enzymatic and enzyme-free methods.

Table 3. Comparison of electrochemical detection of urea using metal oxides and their nanocomposites.

S. No	Electrode Type	Analytical Technique	Enzyme Immobilization Method	Linear Range	Limit of Detection	Real Samples	Ref.
1.	Ni-P	Amperometric	Enzyme free	0.05–11 mM	12 µM	Swimming pool water	[50]
2.	Co-ZIF-NiMWs	DPV	Enzyme free	0.0005–0.5 mM	0.30 µM	Human urine and milk	[52]
3.	NiO/cESM/GCE	SWV	Enzyme free	0.05–2.5 mM	~20 µM	Tap water	[53]
4.	$NiCo_2O_4$ NWs/GCE	CV	Enzyme free	0.01–5 mM	1.0 µM	-	[55]
5.	$Ni(OH)_2$/GCE	CV and DPV		25–90 µM	1.701 µM	-	[56]
6.	Ur/NiO/ITO/glass	CV	Enzymatic	0.83–16.65 mM	0.28 mM	-	[57]
7.	NiO/cellulose/CNT	Chronoamperometric	Non-enzymatic	0.01–1.4 mM	7 µM	Urine	[42]
8.	Vitamin C based NiO/GCE	Amperometry	Non-enzymatic	100–1100 µM	10 µM	Mineral, river, and tap water	[58]
9.	NiO/CTAB/GO/GCE	Amperometry	Non-enzymatic	100 –1200 µM	8 µM	Mineral, river, and tap water	[59]
10.	Ni/Au electrode	CV	Non-enzymatic	-	3.35×10^{-2} mM	Urine	[60]

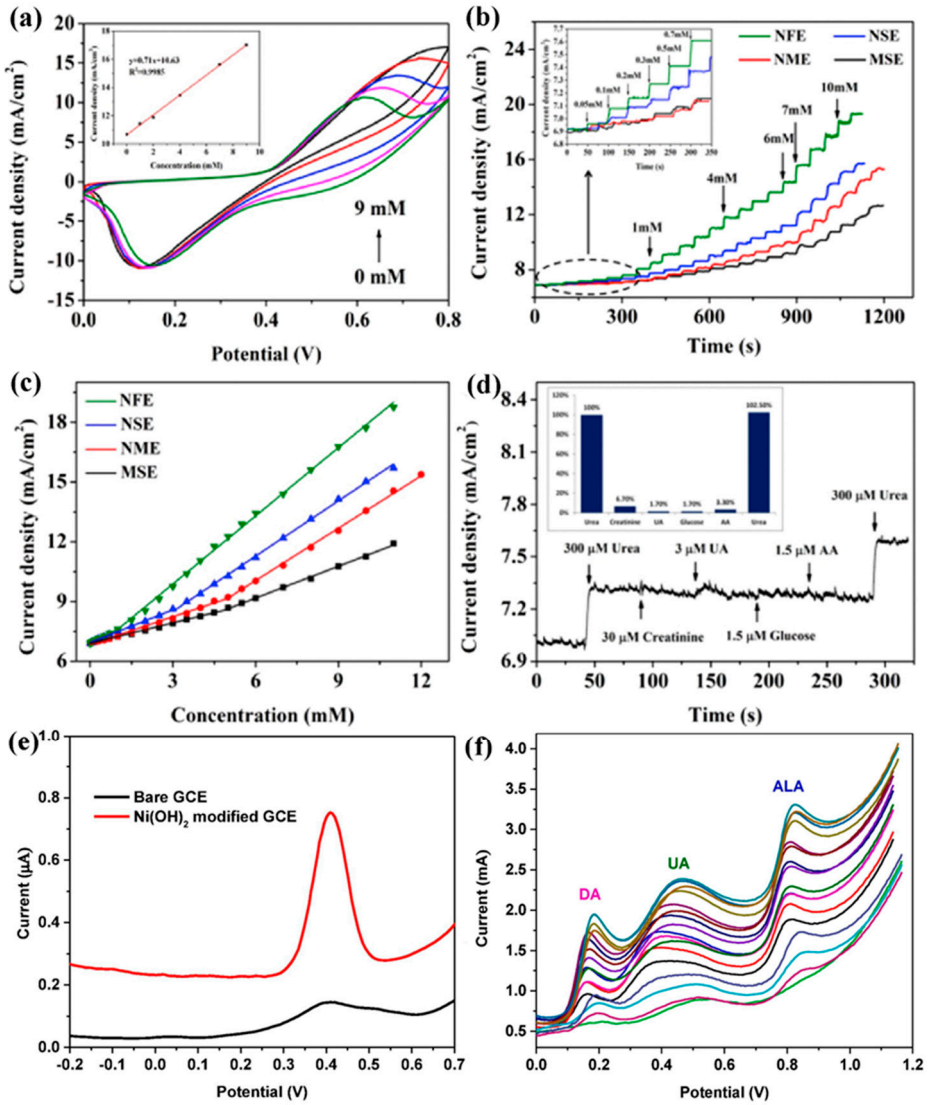

Figure 5. CV profiles of the prepared Ni-P paper electrode (**a**) at different concentrations of urea with a scan rate of 5 mV/s; inset is the plot of oxidation peak currents vs. concentrations of urea, (**b**) amperometric responses of four Ni-P paper electrodes against successive injections of urea, (**c**) calibration curve vs. urea concentrations corresponding to the responses, (**d**) current response to the addition of urea and different interfering species. Reprinted with permission from reference [50] and the corresponding copyright is 2019 Elsevier, (**e**) DPV curve showing the current obtained with bare GCE and $Ni(OH)_2$ modified GCE as the working electrode in a 1 mM solution of UA, and (**f**) DPV curves of $Ni(OH)_2$ nanosheets for simultaneous detection of UA at different concentrations. Reprinted with permission from reference [56] and the corresponding copyright is 2022 Elsevier.

3.2. Graphene and Its Nanocomposites for NOC Sensing

In the last few decades, there has been an increase in the use of multifunctional two-dimensional nanostructure materials, which have the potential to attract exceptional attention due to their physical, chemical, mechanical, and electrical properties. The first successful micromechanical exfoliating method for single-layer graphene was developed by Geim and Novoselov in 2004 [61]. However, certain features, like the number of stacked layers existing in the exfoliation, determine the bandgap and conductivity properties of the graphene. Notably, there are five factors that influence the sensing applications of graphene: electrical conductivity, surface area, thermal stability, low electrical noise, and mechanical properties [62] (Figure 4b). The electrical conductivity of graphene nanostructures has

high carrier mobility and density, even at room temperature, which is advantageous in the fabrication of precious and high-performance electro-analytical devices. In addition, the high surface-to-volume ratio of the graphene allows it to accommodate various receptors for target analytes through van der Waals force, electron transfer, and covalent bonding [63]. Furthermore, the quality of the graphene crystalline lattice can reduce the electrical noise compared with one-dimensional nanostructures. Finally, the mechanical properties of graphene lead to its flexibility and stretchability for use in wearable electronic applications [64]. Sha, R. et al. demonstrated the electrochemical deposition of graphene-polyaniline composites on the glassy carbon electrode (Gr-PANi/GCE) as an affordable method for enzyme-less detection of urea. The observed reduction current in this device shifts towards the positive side during the addition of urea. The electrocatalytic performance of urea at the surface of Gr-PANi/GCE film contains polyanion as an electroactive at neutral pH, whereas Gr flakes, which are highly oxidized, cause a negative charge and play a major role in urea sensing. The decrease in the current due to the interaction between the ions and pi-electrons results in excellent sensitivity and selectivity towards urea [23]. An electrocatalytic material of nickel@carbon nanorod (Ni@CNRs) composite has been prepared by Liu, B.T. et al. using pyrolysis of nickel-based coordination compounds and drop casting on the GCE (Figure 6a–d). The construction of this hybrid structure led to a high surface area along with a homogeneous distribution of Ni on the surface of the structure. Introducing a nickel nanoparticle onto the CNR surface may increase the active region despite its homogeneous distribution. This increase in active region may reduce the distance between Ni nanoparticles and CNRs, thereby enhancing the electron migration rate. These peak (i.e., oxidation current) shifts might be caused by the overlap of the 3d and 4s bands in nickel. In particular, some of the valence electron enter the 3d bands, whereas others enter the 4s bands, as a results holes are generated in the d band. The metal's ability to receive external electrons during the electrochemical process may be facilitated by the presence of d-band holes. These results show that Ni@CNRs significantly enhance the electrocatalytic performance of an electrode by changing the oxidation potential of uric acid [65]. Electrodeposition of Ni/rGO nanocomposites on the conductive carbon fabric (CCF) was fabricated as a wearable electrode by Singh, A. et al. for the enzyme-free detection of uric acid in sweat (Figure 7a–c). Remarkably, the modified Ni/rGO/CCF electrode can act both as a source of electrons and as a reaction site, and hence it can reduce itself to oxidize the uric acid. This phenomenon is due to the synergetic effect of Ni and rGO on enhancing the electron transfer rate, leading to an increase in the electrocatalytic activity. These results revealed that the Ni/RGO/CCF electrode facilitates the selective detection of UA in human sweat [66]. Naik, T. S. K. et al. studied the hydrothermal method used to make non-enzymatic nickel sulfide (NiS) on graphene (NiS/GO), and the product is further coated on the GC. The presence of GO can enhance the electron transfer rate in the matrix of the working electrode and contributes to the electrochemical sensing of urea (Figure 8a–e). For these things to happen, the possible mechanism is as follows: the potential is applied to Ni^{2+} species that underwent oxidation, followed by the oxidation of Ni^{3+} that can be rehabilitated during the forward scan. This Ni^{3+} is favored to oxidize the urea by converting to the Ni^{2+} state via the electron transfer process. Hence, the fabricated NiS/GO/MGCE electrode enhances the conductivity at the surface electrode interface as a result of the diffusion-controlled process, with and without interference, for the determination of urea [67]. Nia, S. M. et al. prepared nickel-manganese oxo/hydroxo nanoparticles on the GO nanocomposites, which were synthesized via a hydrothermal reduction technique. The obtained $Ni(OH)_2/Mn_3O_4$/rGO/PANi nanocomposites were used to modify the screen-printed electrodes for the highly sensitive enzyme-less detection of urea. These studies demonstrated that the prepared nanocomposite has the potential to decrease GO functionalities to enhance sensitivity and inhibit the protonation of aniline via graphene structure [68]. Two-dimensional free-standing NiO nanosheets were synthesized using GO paper as a sacrificial template in another study. In the presence of an alkaline medium, electrochemical studies were conducted, which indicated the high stability and

electrocatalytic oxidation of urea as well as interferent agents resulting in non-enzymatic sensing of urea. The possible sensing mechanism is that urea can absorb Ni^{3+} ions, which certainly decreases its cathodic peak current. On the other hand, urea would induce the adsorption of oxides intermediated through the active surface sites of the NiO nanosheets. Thus, urea may restrict the kinetics of the redox reaction and cause a positive shift in the anodic peak current that indicates improved sensitivity, quick response time, and good stability [69]. Mohiuddin, A. K. et al. demonstrated the creation of a defect site on nickel-cobalt double-hydroxide decorated graphene ($Co_xNi_{1-x}(OH)_2$/G) using the hydrothermal method. These defect sites can act as superior active sites for the enzyme-free detection of uric acid. The $Co_xNi_{1-x}(OH)_2$ creates a defect and reduces the charge transfer resistance of $Ni(OH)_2$, thus actively participating in the redox reaction. Then, the graphene reduces the aggregation of $Co_xNi_{1-x}(OH)_2$, which improves the electroactive surface region and enhances the electrical conductivity of nanocomposites [70]. The literature also shows that an electrochemical deposition of ITO/PDPA (poly-diphenylamine)/PTA (phosphotungstic acid)/Gra-ME electrode has been designed for its electrochemical activity towards urea detection. Upon increasing the concentration of urea, the oxidation peak current also rises, and the amperometric response of the ITO/PDPA/PTA/Gra-ME-based electrode with the addition of urea shows enhanced electrocatalytic activity. This enhancement is ascribed to the synergistic interaction of sandwiched PDPA/graphene, whereas the tungsten atoms provide fast reversible multi-electron redox behavior that augments the fast electron transfer rate, resulting in improved sensitivity [71]. N-doped graphene nanosheets are prepared by microwave irradiation and subsequently coated onto the glass carbon electrode for the non-enzymatic detection of uric acid in human blood samples (Figure 9a–e). The well-organized oxidation peak is co-related with the higher electrocatalytic activity observed, owing to the nitrogen atom in the N-doped graphene nanosheets interacting with uric acid via a hydrogen bond. This bond may activate hydroxyl and amine groups in uric acid, thus enhancing the electron transfer process using these N-doped graphene [72] nanosheets. A detailed comparison of the literature that pertains to NOC sensors based on graphene and its nanocomposites is given in Table 4.

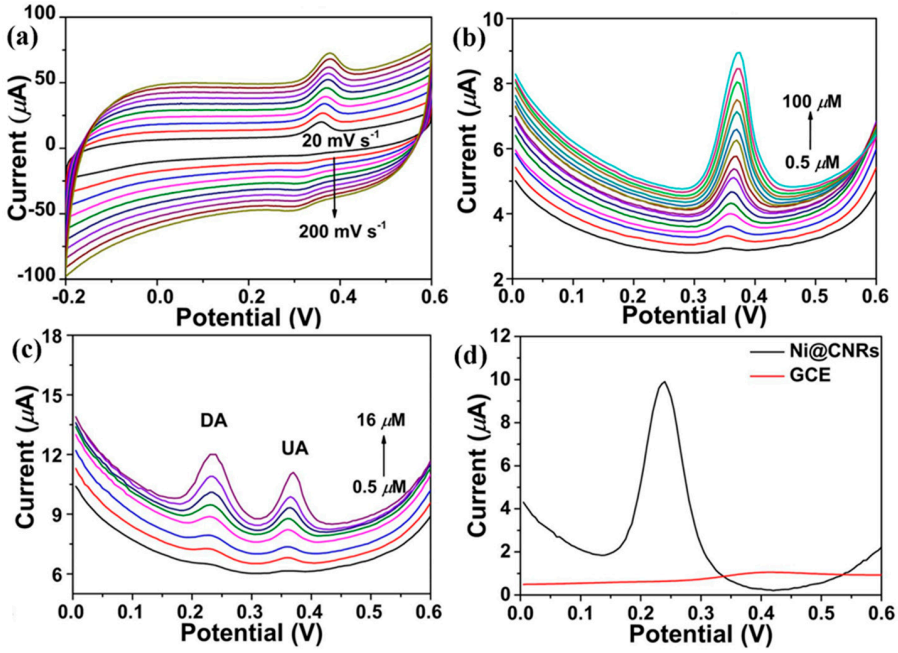

Figure 6. CV curves of Ni@CNRs@GCE with (**a**) 100 µM UA with different scan rates, (**b**) DPV curves with different concentrations, (**c**) simultaneous detection of UA with different concentrations, and (**d**) 100 µM UA. Reprinted with permission from reference [65] and the corresponding copyright is 2021 Elsevier.

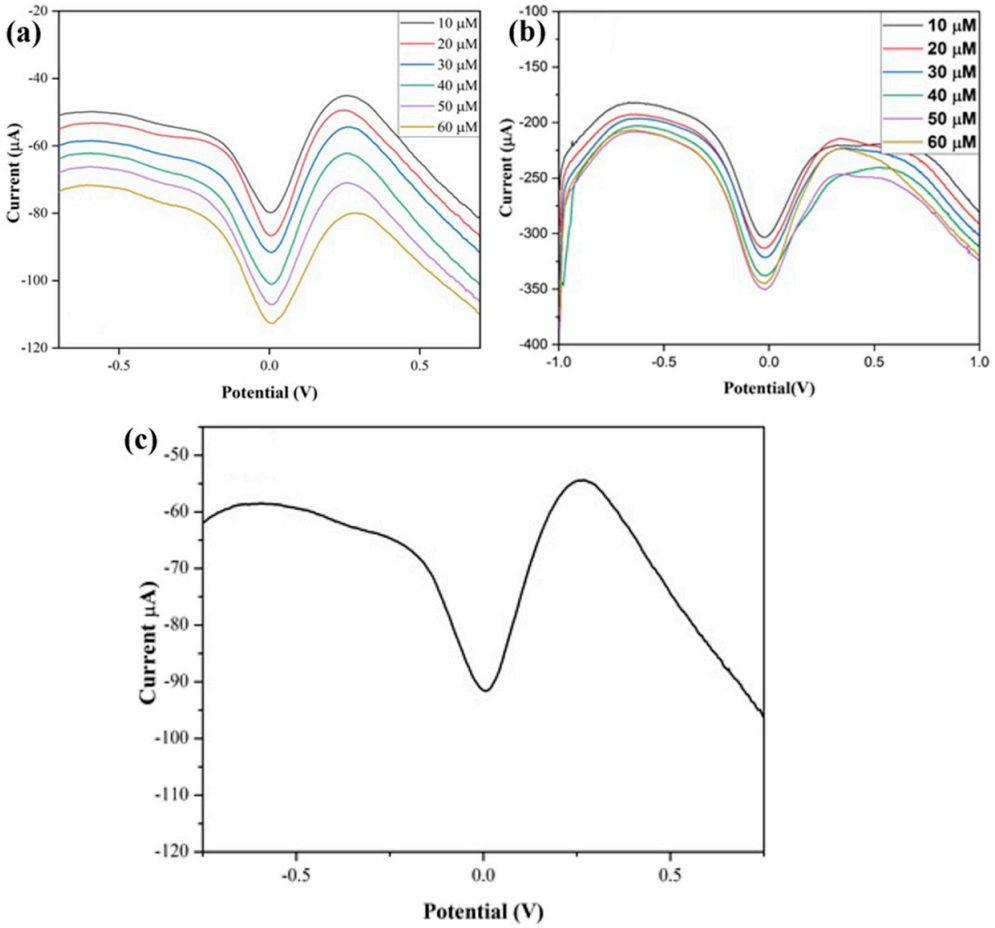

Figure 7. DPV of Ni/RGO/CCF (**a**) at different concentrations of UA, (**b**) on a real sample of human sweat with known urea concentrations, and (**c**) with UA in 20 µL sweat. Reprinted with permission from reference [66] and the corresponding copyright is 2022 Elsevier.

Table 4. Comparison of electrochemical detection of urea using graphene and its nanocomposites.

S. No	Electrode Type	Analytical Technique	Enzyme Immobilization Method	Linear Range	Limit of Detection	Real Samples	Ref.
1.	Gr-PANi/GCE	I–V	Non-enzymatic	10–200 µM	5.88 µM	Milk and tap water	[23]
2.	Ni@CNRs	DPV	Enzyme free	35–100 µM	0.166 µM	Human urine	[65]
3.	Ni/RGO/CCF	DPV	Enzyme free	10–60 µM	5.083 µM	Human sweat	[66]
4.	NiS/GO/MGCE	CV	Enzyme free	0.1–1.0 mM	3.79 µM	Milk	[67]
5.	$Ni(OH)_2/Mn_3O_4$/rGO/PANi	CV	Enzyme free	30 µM–3.3 mM	16.3 µM	Human serum	[68]
6.	2D NiO papers	i-t	Enzyme free	4.4–181.6 mM	2 µM	-	[69]
7.	$CoxNi1-x(OH)_2$/G/GCE	DPV	Enzyme free	0.25–925 µM	0.097 µM	Urine	[70]
8.	ITO/PDPA/PTA/Gra-ME nanohybrid	CV	Enzyme free	1–13 µM	-	-	[71]
9.	NG	CV	Enzyme free	0–600 µM	0.0045 µM	Serum	[72]
10.	GND/PANI/urease	I–V	Enzymatic	0.1–0.9 mg mL^{-1}	0.05 mg mL^{-1}	-	[73]
11.	Graphene nanoplatelet/graphitized nanodiamonds nanocomposite	I–V	Enzymatic	0.1–0.9 mg mL^{-1}	5 µg/mL	-	[74]
12.	$NiCo_2O_4$/3D graphene/ITO	Chronoamperometric	Non-enzymatic	0.06–0.30 mM	5.0 µM	Urine	[75]
13.	NiS/GO/MGCE	CV	Non-enzymatic	0.1–1.0 mM	3.79 µM	Milk	[67]

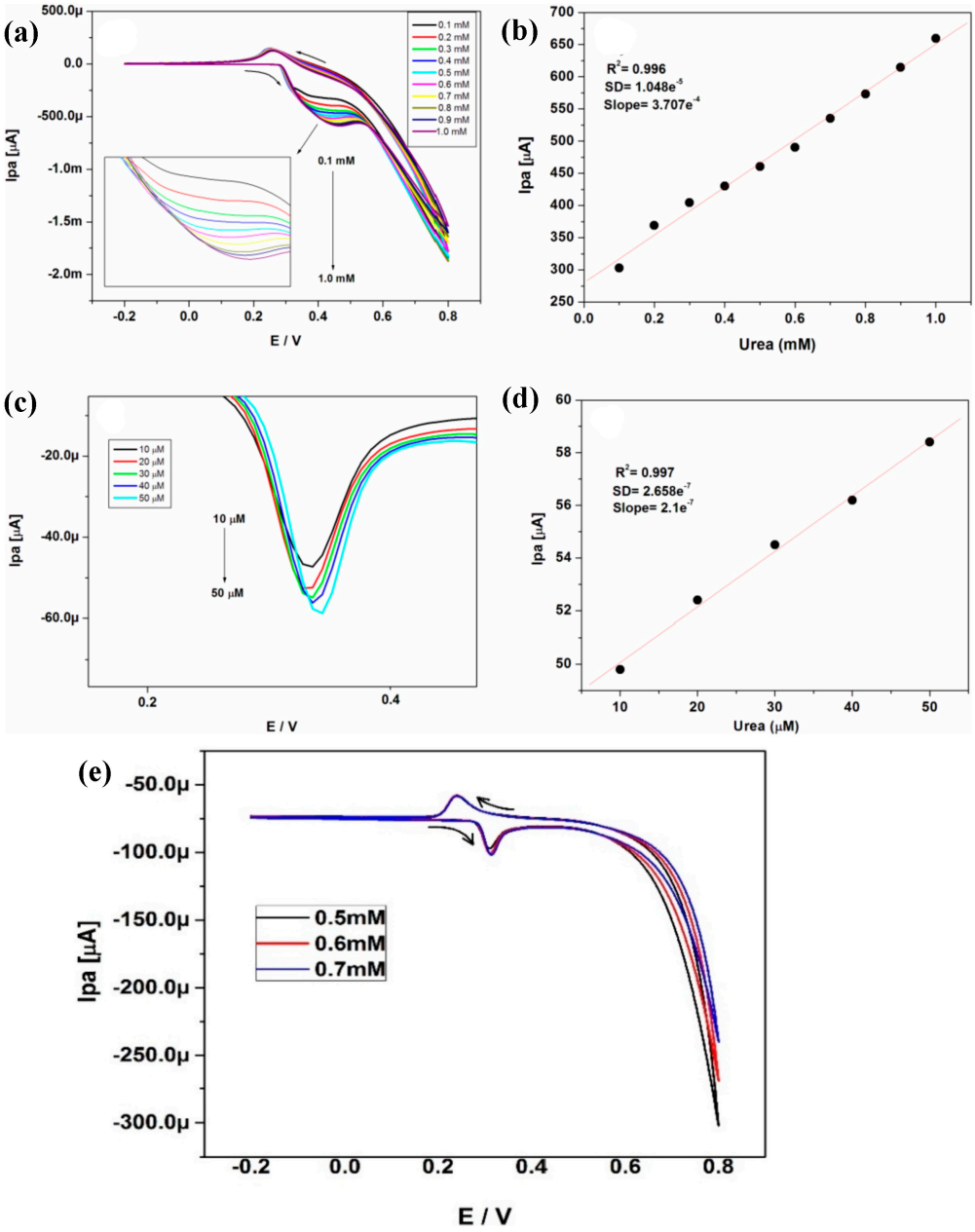

Figure 8. (**a**) CV curve for various urea concentrations (0.1–1.0 mM) detected using NiS/GO/MGCE, (**b**) anodic peak current against concentration, (**c**) DPV curve for urea at different concentrations (10–50 µM), (**d**) anodic peak current against concentration, and (**e**) CV curve of a milk sample spiked with different concentrations of urea on NiS/GO/MGCE. Reprinted with permission from reference [67] and the corresponding copyright is 2020 Elsevier.

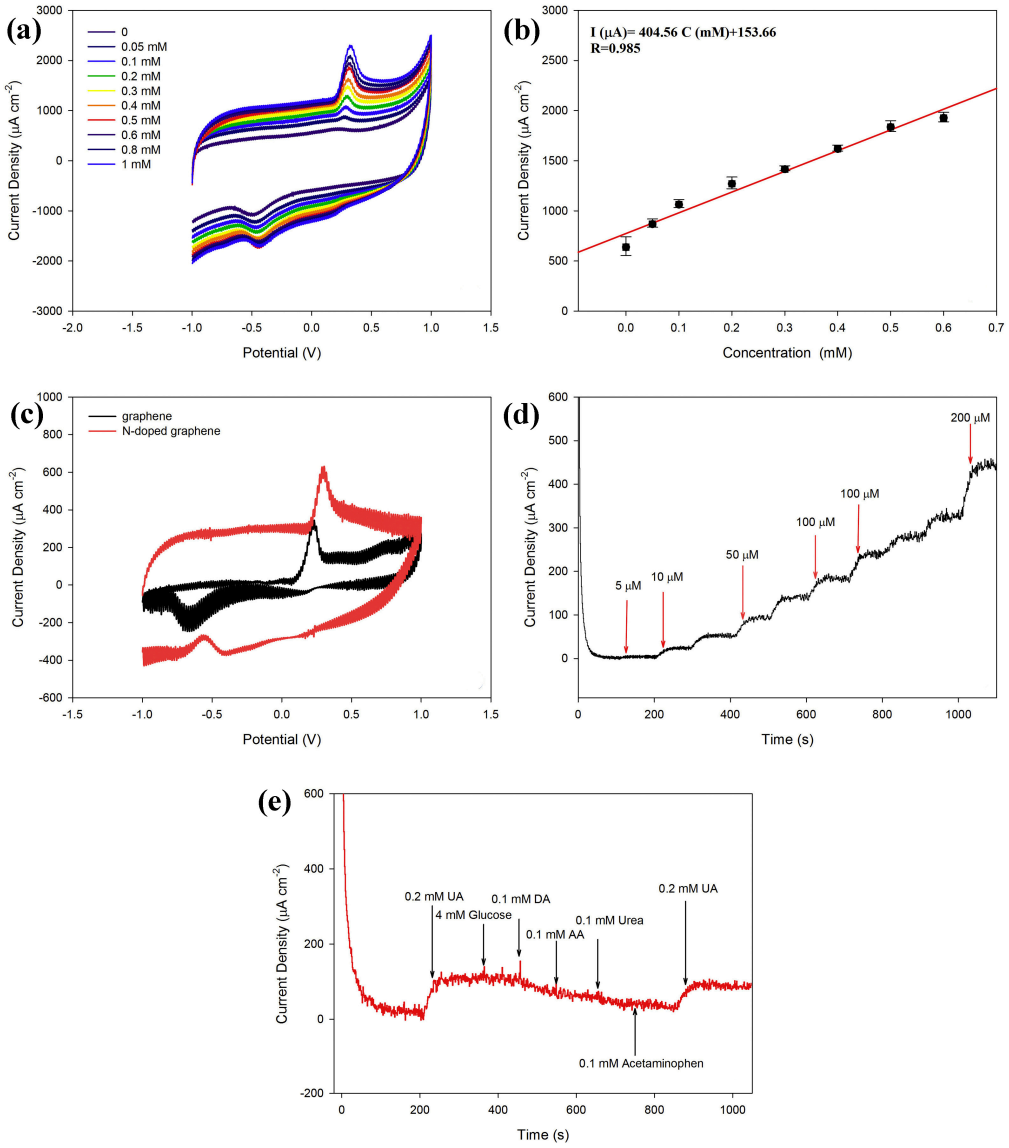

Figure 9. (**a**) CV curve of the N-doped graphene electrode at different concentrations of UA, (**b**) linear fit of current vs. concentration of UA, (**c**) CV curve of the neat graphene and N-doped graphene electrodes after subtracting the background in 0.1 M phosphate buffer (PB) containing 0.2 mM UA, (**d**) amperometric response of the N-doped graphene modified electrode with subsequent infusion of various concentrations of UA, and (**e**) amperometric response of the N-doped graphene electrode toward UA under the effect of different interferents. Reprinted with permission from reference [72] and the corresponding copyright is 2018 Elsevier.

3.3. Field-Effect Transistors (FET)

Using state-of-the-art technology for the fabrication of a low-cost chip-based device called a field-effect transistor (FET) has been demonstrated on a flexible substrate for biosensing applications. Recently, disposable chip sensors have been suggested for real-time diagnosis, in particular, in laboratory-less and non-invasive methods [76]. The field-effect transistor (FET) is an advanced device in which special classes of sensors are used. Biomolecule analysis is one of the many analyses that can be performed using this device, and the device has great use in biomedical applications due to its ability to be a miniaturized device. So, FET requires a very small concentration of specimens, such as serum, blood, or urine [77]. Meanwhile, the electrochemical detection method has been used either by an ion-sensitive electrode or by a field-effect transistor for biochemical sensors (Figure 10a,b). Initially, FET was developed in 1970 by P. Bergveld, followed by its development in 1983

by J. van der Spiegel et al., who first reported an extended-gate ion-sensitive field-effect transistor [78]. In 1997, Pijanowska and Torbicz reported the immobilization of urease on the silicon nitride surface for the detection of urea [79]. In recent times, to fabricate molecularly imprinted polymers (MIP), the photopolymerization method has been considered for constructing an ISFET device, which was developed by Rayanasukha, Y. et al. In this non-enzymatic detection of urea, polymethyl methacrylate (PMMA) and urea are used as polymer membranes and templates, respectively. The MIP-modified ISFET sensor has been optimized by changing features like the thickness of the polymer membrane, the ratio of polymer to urea in the composite, and the incubation time. The electrochemical response of the fabricated MIP-modified electrodes can attain the highest response rate with respect to concentrations (Figure 11). Moreover, the fabricated MIP-modified ISFET possesses high selectivity, good reproducibility, and repeatability. Hence, this ISFET would be a reliable device for the non-enzymatic detection of urea [80]. In addition, a proof-of-concept based SnO_2:F device was constructed on an FTO-coated glass substrate, which can act as an extended-gate ion-sensitive field effect transistor (EG-FET). Drain-source current (I_{DS}) was measured as a function of drain-source voltage (V_{DS}) with a fixed Vref voltage. Notably, I_{DS} was measured as a function of Vref with a fixed V_{DS} voltage. The changes in V_{FB} can be indirectly detected with respect to the shift in threshold voltage, which is proportional to the number of charge carriers that have been absorbed over the oxide surface. The enzymatic field-effect transistor sensor response (I_{DS}) has been measured with varying urea concentrations, and the voltage has been fixed, and the I_{DS} was measured as a function of time. To determine the sensing performance of the device, the measurements were carried out at different pHs and buffer concentrations. Hence, this proposed method may pave the way for a new class of sensors for clinical diagnosis [81]. A back-gated field effect transistor (BG-FET) was fabricated as a point-of-care (POC) for the detection of urea in a human urine sample. The spin coating method was used to allow the BG-FET to analyze urea. In this method, PMMA is used as a dielectric layer, CdS-TiO_2 nanocomposites are used as a channel layer, and silver paste is used to make a conductive electrode. The hydrolysis of urea in the presence of urease selectively produces ammonium ions, which were sensed by the BG-FET. As a result, there was an increase in drain current in the BG-FET, with a higher number of charge carriers being generated when ammonia was absorbed on CdS-TiO_2 nanostructures. To this extent, changes in the measurable signal would be standardized to selectively measure the activity of different types of gas/vapor. The proposed BG-FET sensor design would use real-time, highly sensitive, and selective detection of urea in excretory metabolites, that can be suitable for developing a POC device [82].

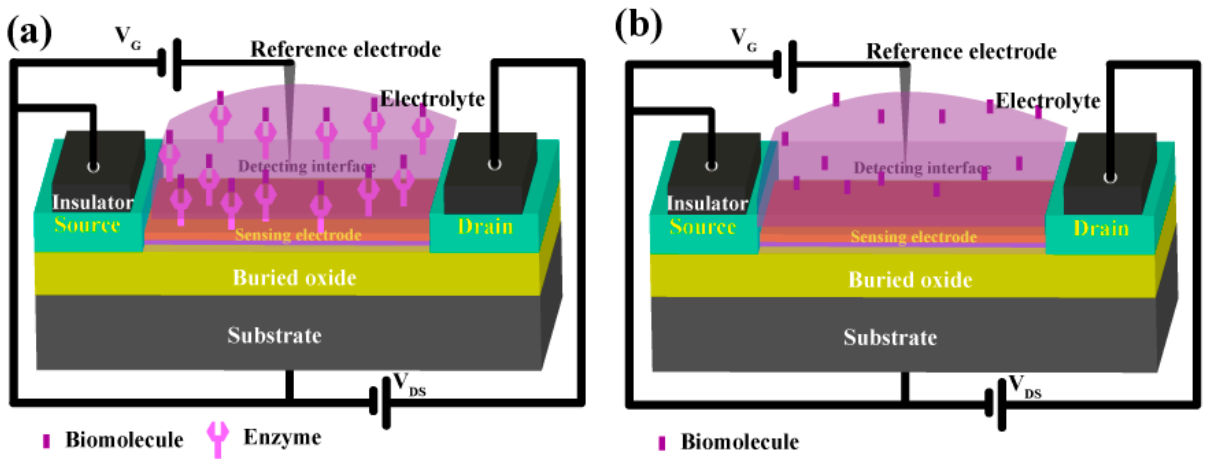

Figure 10. Construction of a field effect transistor (FET)-based device for (**a**) enzymatic and (**b**) enzyme-free detection of NOCs.

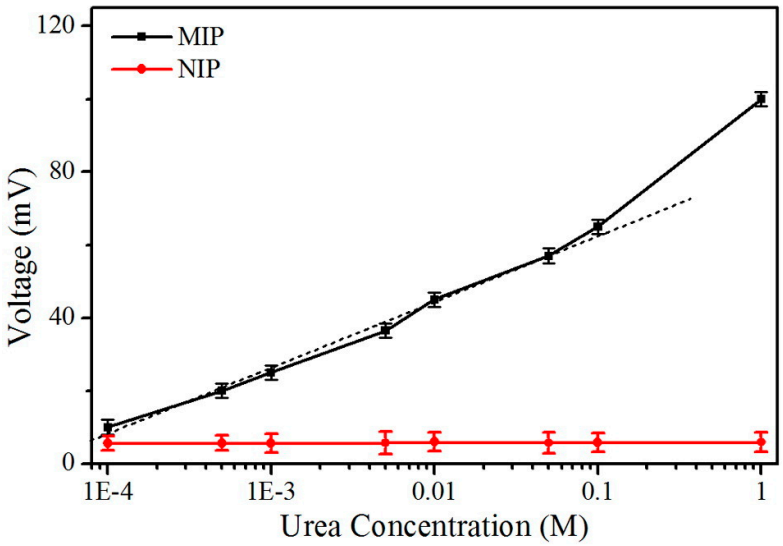

Figure 11. Voltage response of MIP (black line) and NIP (red line) modified ISFET sensors in different urea concentrations (the dotted line is the trend line). Reprinted with permission from reference [80] and the corresponding copyright is 2016 Elsevier.

3.4. Printed Electrodes

As the demand for affordable devices has increased, a simplified fabrication process has been introduced via printing or painting technology to fabricate disposable, flexible, and wearable functional devices [83]. A prototype device has been demonstrated using these techniques for various chemical sensing applications [84]. Nanomaterials contain more active sites at their surface with a high surface area that favors enhanced electron carrier mobility and density. This property is more important in electrically transduced sensing devices. So, printed electrode-based electrically/electrochemically transduced devices have desirable features like affordability, sensitivity, specificity, limit of detection, and reliability (Figure 12) [85]. The first printed electronics were successfully commercialized in household appliances from 1948 to 1960 [86]. In 2011, the first inkjet-printed flexible electronic devices were invented by Massachusetts Institute of Technology (USA) researchers, resulting in more attention among the research community for developing a printed electrode as a device for the detection of various components [87]. In the modern era, metals and metal oxides, carbon derivatives, and conductive polymers are used as ink to fabricate printed electrode-based devices for sensor applications. Hassan, R.Y. et al. studied a conductive polymer/MWCNT nanocomposite coated on the screen-printed electrode (SCE) by drop casting and then used it to detect urea in blood samples. The conductive polymer of poly(o-toluidine) (PoT) was prepared via an oxidative polymerization reaction and was used to fabricate an enzymatic MWCNT/PoT/SCE electrode. The direct electrocatalytic oxidation of the enzymatically produced ammonium ions was obtained using hybrid multi-walled carbon nanotubes and their nanocomposite of PoT (MWCNT/PoT) that can be used for detection of urea in real human blood samples [88]. Electropolymerizing on the molecularly imprinted membrane with a low-cost, flexible urea-PEDOT/c-Au nanotube sensor was used to detect urea via epidermal analysis. The obtained flexible EC sensor was attached to the wrist to absorb urea via sweat, and it was observed that the measurable signal changes as the concentration of urea increases. In human sweat, various substances are present, among which a few have EC activity or are more or less identical in structure to urea. Therefore, it can be a promising method for the efficient, rapid, and non-invasive determination of urea in real sweat samples [89]. The fabrication of urease-MBs/GO/NiO has been performed on the PET substrate using sputtering and screen-printing technology. The electrode surface was functionalized with APTES, and in this, MBs (i.e., magnetic beads) were used to enhance the chemical bonding, thus improving the electrocatalytic performance. The sensing characteristics of urea biosensors have been measured with a

voltage-time (V-T) method for MBs/GO/NiO films with low response times, which show excellent charge transition capability. However, there has been a drift effect observed in these biosensors, which might be attributed to the process of adsorption and desorption of the ions and other factors, such as temperature instability, solution contamination, or material decomposition within the sensor, as studied by Chou, J.C. et al. [90]. Berto, M. et al. demonstrated that a fully printed PEDOT: PSS- based organic electrochemical transistor (OECT) has been developed in which the PEDOT: PSS layer acts as a channel and gate layer, respectively. The response of the device is determined by the changes in channel conductivity caused by the ionic species generated during urea hydrolysis catalyzed by the entrapped urease. Screen-printing flexible electrodes using the OECT method is a fascinating technique for large-scale and cost-effective production of point-of-care devices [91]. The screen-printing method, developed by Bao, Q. et al., was used to make a modified multiwalled carbon nanotube/polyaniline (MWCNT/PANi) composite device. The electrical conductivity increased during the polymerization, which was caused by doping with H+. Further, H+ was unbiased from PANi when introducing the urea, resulting in a decrease in the conductivity of PANi and a measurable signal being acquired. With the addition of MWCNT to the PANi chain, there is a formation of conduction channels that causes smooth transduction of electrical signals into measurable signals due to the low conductivity of PANi. Therefore, the modification of the MWCNT/PANi composite significantly enhances the sensitivity for the detection of urea in an enzyme-free method [92]. A detailed comparison of the literature related to NOC sensors made with printable electrodes is given in Table 5.

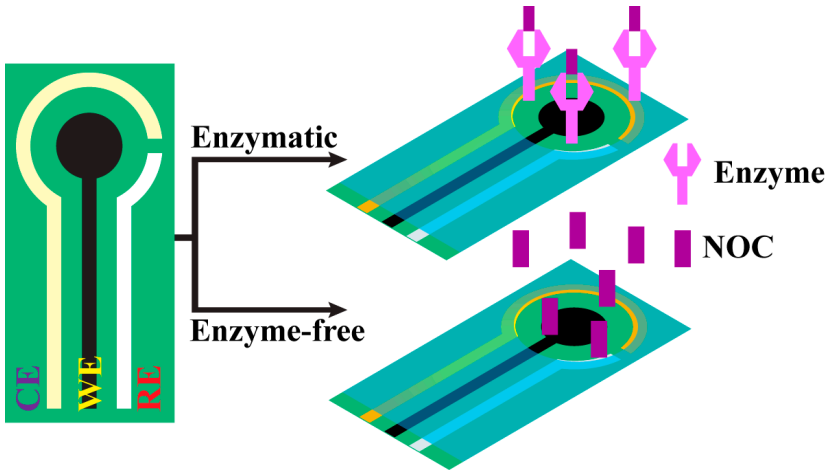

Figure 12. Fabrication of printed electrodes for the detection of NOCs with enzymatic and enzyme-free methods.

Table 5. Comparison of electrochemical detection of urea using printed electrode devices.

S. No	Electrode Type	Enzyme Immobilization Method	Linear Range	Limit of Detection	Analytical Technique	Real Samples	Ref.
1.	MWCNT/PoT/SPE	Enzymatic	0.1–11 mM	0.03 mM	CV	Human blood	[88]
2.	PEDOT/C-Au NTs EC	Non-enzymatic	1−100 mM	-	DPV	human sweat	[89]
3.	Urease/MBs/GO/NiO	Enzymatic	1.665–8.325 mM	0.223 mM	V-T	-	[90]
4.	OECTs	Enzymatic	1 µM–10 mM	1 µM	I-V	-	[91]
5.	MWCNT/PANi-modified SPCE	Non-enzymatic	10–50 µM	10 µM	CV	-	[92]

3.5. Electrochemical Impedimetric Detection of NOCs

Electrochemical impedimetric spectroscopy (EIS) [93] can sensitively monitor changes caused by capacitance or charge transfer resistance during the specific binding of targeted elements [94]. As per the operational principle and mechanism of the measurement, EIS

instruments have been differentiated into two types: non-faradaic EIS (i.e., impedimetric transducers) and faradaic EIS (i.e., amperometric and potentiometric transducers). First, the non-faradaic EIS is a non-destructive method as it favors persistent measurement on the same samples. EIS is also performed at various frequency ranges, and it is highly sensitive to even very small changes in the measurement [93,95]. The EIS analysis does not involve any redox reaction and there is no need for direct current or a reference electrode, whereas the faradaic EIS is very focused on electrochemical reactions and provides specific information that does not require multiple frequency sweeps and results in rapid (i.e., less time-consuming) measurements. Faradaic EIS approaches can be employed wherever non-destructive measures are not a priority. So, non-faradaic and faradaic EIS-based detections are more amenable to fabricating a miniaturized kit, in terms of sensitivity, data complexity, and a non-destructive nature [96,97]. Recently, Tammam, R. H. and Saleh, M. M., synthesized a different weight percentage of NiOx on GCE and measured it in an alkaline medium. The fitted Randles equivalent circuit reveals a double-layer capacitor (C_{dl}) due to the inhomogeneity and roughness on the surface of the electrode. This capacitor's presence can be attributed to the increase in the concentration of $Ni(OH)_2$ and NiOOH with the increase in the loading percentage. However, R_{ct} decreases due to the faster charge transfer of the redox couple of $Ni(OH)_2$/NiOOH, thus converting the fraction of the α-$Ni(OH)_2$ species to β-$Ni(OH)_2$. Further, this conversion inhibits the diffusion of -OH ions onto the electrode surface. Then, upon increasing the urea concentration, the R_{ct} decreases, which may be attributed to an increase in the charge transfer kinetic due to the higher electrocatalytic oxidation of urea. At higher urea concentrations, the oxidation of Ni (II) to Ni (III) is accelerated. Hence, Ni (III) is removed by urea, which enhances further conversion of Ni (II) to Ni (III), resulting in an increased charge transfer rate caused by the conversion of the OH^- ions to CO_3^{2-} ions and a CO_2 byproduct [51]. Goda, M.A. et al. demonstrated the R_{ct} measurement for the NiOx/CuOx/PANI/GC electrode during the electrocatalytic oxidation of urea. The fabricated catalyst exhibits a significant decrease in R_{ct}, indicating faster charge transfer of NiOx/CuOx/PANI/GC catalysts due to their higher electrocatalytic performance. This may be due to the conductivity contribution of the PANI polymer layer beneath the bimetallic catalyst layer [54]. Salarizadeh, N. et al. developed a NiO-MoO_3 on GCE, and the EIS results indicate that the R_{ct} value is lower than that of the bare GCE in the presence of urea (Figure 13a). As a result, there was a growth in the reaction rate at the electrode interface. Thus, the decrease in R_{ct} value significantly proves the electroactivity of the developed electrode for the oxidation and enzyme-free detection of urea [98]. Then, electrospun ferric ceria nanofibers were mixed with MWCNTs coated on the surface of GCE by Shekh, M.I. et al. The R_{ct} value was estimated for the MWCNT70@CeO_2, MWCNT70@FC-1, and MWCNT70@FC-2 tested in the presence of uric acid. Amongst these materials, MWCNT70@FC-2 attained the lowest R_{ct} value for the detection and oxidation of uric acid (Figure 13b). This lowest value is because of the sufficient weight percentage of MWCNT (i.e., 70%) and Fe^{3+} (i.e., 30%) leading to exceptional electrocatalytic performance for the detection of uric acid [99]. Albaqami, M.D. and his colleagues grew Co_3O_4 nanowires on cotton silk. Then, they drop-casted uricase onto the Co_3O_4 nanostructures on the GCE surface. This fabricated electrode was used to detect uric acid. The fabricated electrode exhibits a higher charge transfer rate, and a small, semicircular Nyquist's plot of the electrode shows that the nanowires provide a better measurable electrical signal than that of a platelet-like nanostructure. However, immobilization of uricase can slightly influence impedimetrics due to its insulating features in the presence of an enzyme. Hence, the researchers suggested that the proposed nanowire be used for the determination of uric acid because the cotton silk acts as a co-catalyst to boost the electroactive behavior [100].

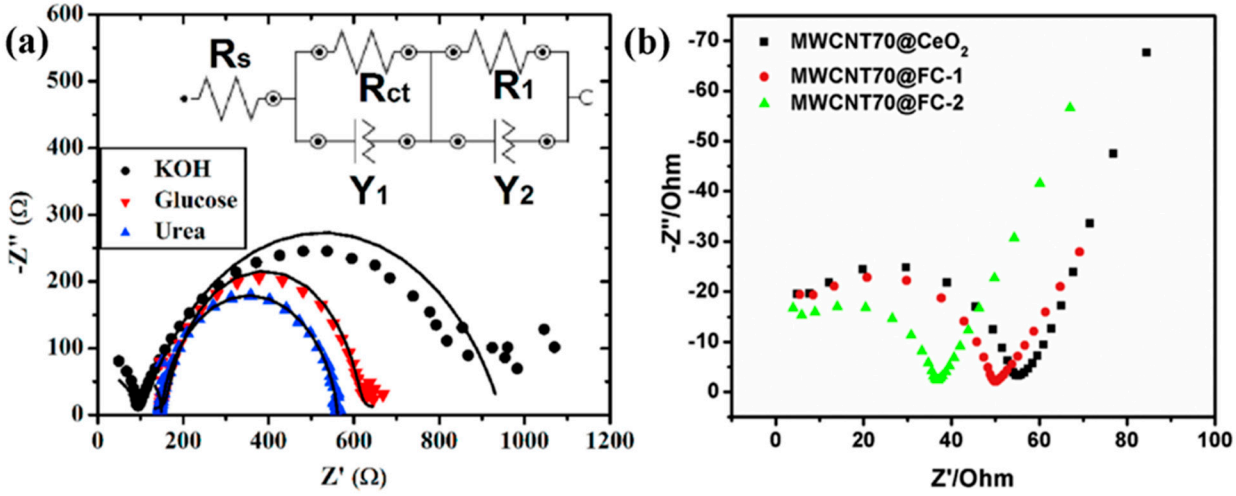

Figure 13. EIS plots of (**a**) NiO–MoO_3 with the presence of 1 mM urea (blue color) (Inset: Equivalent circuit). Adapted from reference [98] and the corresponding copyright is 2022 Elsevier, and (**b**) the modified GCE with MWCNT70@FC-2 measured in 0.1 M PBS solution containing 0.01 M UA (pH = 6.0) in the frequency region of 1–10 Hz with 50 mV amplitude (Green color). Reprinted with permission from reference [99] and the corresponding copyright is 2020 Elsevier.

4. Conclusions and Future Perspectives

The development of biosensors using advanced nanomaterials for the detection of NOCs shows desirable sensor characteristics, such as sensitivity, selectivity, limit of detection, and stability. The incorporation of nanoscale materials, such as nickel nanoparticles, graphene, and their nanocomposites, into biosensors has been elaborated. Devices like FET and printed electrodes have revealed the capabilities of a wide range of NOC detection methods and confirmed that extensive and elevated sensing performance has been achieved. The advantages of nanomaterials in the field of sensors make them a new and unavoidable platform for the sensitive analysis of NOCs. These nanomaterials can provide a potential solution not only for biomedical or clinical analysis but also in the fields of agricultural pesticides, environment, and dairy product detection. In this review, we have elaborately discussed the recent advances in the sensing of NOCs using various nanocomposite electrodes with or without functionalization using an enzymatic and/or enzyme-free detection method. A good sensing platform needs to be made as a rapid sensing element that can be used to detect NOCs in real samples in a selective, cheap, disposable, and flexible way. However, the major challenge in this research field is the development of nanomaterials on paper and textile fabrics as microfluidic point-of-care (μ-POC) devices. The state-of-the-art technology in biosensors has been envisioned to construct and develop a selective separation followed by detection of various biomolecules. This detection creates a new roadmap towards the development of affordable, rapid response, wearable, and on-site diagnosis kits in the future.

Author Contributions: M.J.—Conceptualization and Writing original draft, D.D.—Review & editing, A.R.R.—Review and validation, S.C.—Review, editing, funding acquisition & supervision. All authors have read and agreed to the published version of the manuscript.

Funding: This work was supported by the National Research Foundation of Korea (NRF) grant funded by the Korea government (No.2023R1A2C1003669), and the Gachon University research fund of 2023 (GCU-202303970001).

Institutional Review Board Statement: Not applicable.

Informed Consent Statement: Not applicable.

Data Availability Statement: No new data were created or analyzed in this study. Data sharing is not applicable to this article.

Conflicts of Interest: The authors declare no conflict of interest.

References

1. Connor, H. Medieval uroscopy and its representation on misericords—Part 1: Uroscopy. *Clin. Med.* **2001**, *1*, 507. [CrossRef]
2. Simerville, J.A.; Maxted, W.C.; Pahira, J. Urinalysis: A comprehensive review. *Am. Fam. Physician* **2005**, *71*, 1153–1162. [PubMed]
3. Voswinckel, P. From uroscopy to urinalysis. *Clin. Chim. Acta* **2000**, *297*, 5–16. [PubMed]
4. Armstrong, J.A. Urinalysis in Western culture: A brief history. *Kidney Int.* **2007**, *71*, 384–387. [CrossRef] [PubMed]
5. Gardner, K., Jr. The art and gentle science of Pisse-Prophecy. *Hawaii Med. J.* **1971**, *30*, 166–169.
6. Durgalakshmi, D.; Rishvanth, R.; Mohanraj, J.; Aruna, P.; Ganesan, S. A Roadmap of cancer: From the historical evidence to recent salivary metabolites-based nanobiosensor diagnostic devices. *Curr. Metabolomics Syst. Biol. Former. Curr. Metabolomics* **2021**, *8*, 27–52.
7. Babu, K.J.; Senthilkumar, N.; Kim, A. Freestanding and binder free PVdF-HFP/Ni-Co nanofiber membrane as a versatile platform for the electrocatalytic oxidation and non-enzymatic detection of urea. *Sens. Actuators B Chem.* **2017**, *241*, 541–551. [CrossRef]
8. Dhinasekaran, D.; Soundharraj, P.; Jagannathan, M.; Rajendran, A.R.; Rajendran, S. Hybrid ZnO nanostructures modified graphite electrode as an efficient urea sensor for environmental pollution monitoring. *Chemosphere* **2022**, *296*, 133918. [CrossRef]
9. Jakhar, S.; Pundir, C. Preparation, characterization and application of urease nanoparticles for construction of an improved potentiometric urea biosensor. *Biosens. Bioelectron.* **2018**, *100*, 242–250. [CrossRef]
10. Ezhilan, M.; Gumpu, M.B.; Ramachandra, B.L.; Nesakumar, N.; Babu, K.J.; Krishnan, U.M.; Rayappan, J.B. Design and development of electrochemical biosensor for the simultaneous detection of melamine and urea in adulterated milk samples. *Sens. Actuators B Chem.* **2017**, *238*, 1283–1292. [CrossRef]
11. Kumar, V.; Chopra, A.; Arora, S.; Yadav, S.; Kumar, S.; Kaur, I. Amperometric sensing of urea using edge activated graphene nanoplatelets. *RSC Adv.* **2015**, *5*, 13278–13284. [CrossRef]
12. Verma, R.; Gupta, B. A novel approach for simultaneous sensing of urea and glucose by SPR based optical fiber multianalyte sensor. *Analyst* **2014**, *139*, 1449–1455. [CrossRef] [PubMed]
13. Jagannathan, M.; Dhinasekaran, D.; Soundharraj, P.; Rajendran, S.; Vo, D.-V.N.; Prakasarao, A.; Ganesan, S. Green synthesis of white light emitting carbon quantum dots: Fabrication of white fluorescent film and optical sensor applications. *J. Hazard. Mater.* **2021**, *416*, 125091. [PubMed]
14. Mohanraj, J.; Durgalakshmi, D.; Rakkesh, R.A.; Balakumar, S.; Rajendran, S.; Karimi-Maleh, H. Facile synthesis of paper based graphene electrodes for point of care devices: A double stranded DNA (dsDNA) biosensor. *J. Colloid Interface Sci.* **2020**, *566*, 463–472. [CrossRef]
15. Jagannathan, M.; Dhinasekaran, D.; Rajendran, A.R. N-Graphene paper electrodes as sustainable electrochemical DNA sensor. *J. Electrochem. Soc.* **2023**, *170*, 077503. [CrossRef]
16. Aono, T.; Matsubayashi, K.; Kawamoto, A.; Kimura, S.; Ozawa, T. Normal ranges of blood urea nitrogen and serum creatinine levels in the community-dwelling elderly subjects aged 70 years or over–correlation between age and renal function. *Nihon Ronen Igakkai Zasshi Jpn. J. Geriatr.* **1994**, *31*, 232–236. [CrossRef] [PubMed]
17. Burns, C.M.; Wortmann, R.L. Clinical features and treatment of gout. In *Kelley and Firestein's Textbook of Rheumatology*; Elsevier: Amsterdam, The Netherlands, 2017; pp. 1620–1644.e4.
18. Sharfuddin, A.A.; Weisbord, S.D.; Palevsky, P.M.; Molitoris, B.A. Acute kidney injury. In *Brenner Rector's Kidney*; Elsevier: Amsterdam, The Netherlands, 2012; pp. 1044–1099.
19. Cecil, R.L.F.; Goldman, L.; Schafer, A.I. *Goldman's Cecil Medicine, Expert Consult Premium Edition–Enhanced Online Features and Print, Single Volume 24: Goldman's Cecil Medicine*; Elsevier Health Sciences: Amsterdam, The Netherlands, 2012; Volume 1.
20. Laboratories, M.C. Uric Acid. Available online: https://www.mayocliniclabs.com/api/sitecore/TestCatalog/DownloadTestCatalog?testId=8440#:~:text=Males%201%2D10%20years%3A%202.4,are%20%3C12%20months%20of%20age (accessed on 4 September 2023).
21. Laboratories, M.C. Creatinine Test. Available online: https://www.mayoclinic.org/tests-procedures/creatinine-test/about/pac-20384646 (accessed on 2 September 2023).
22. Zhybak, M.; Beni, V.; Vagin, M.Y.; Dempsey, E.; Turner, A.P.; Korpan, Y.B. Creatinine and urea biosensors based on a novel ammonium ion-selective copper-polyaniline nano-composite. *Biosens. Bioelectron.* **2016**, *77*, 505–511. [CrossRef]
23. Sha, R.; Komori, K.; Badhulika, S. Graphene–polyaniline composite based ultra-sensitive electrochemical sensor for non-enzymatic detection of urea. *Electrochim. Acta* **2017**, *233*, 44–51. [CrossRef]
24. Ning, Y.-N.; Xiao, B.-L.; Niu, N.-N.; Moosavi-Movahedi, A.A.; Hong, J.P. Glucose oxidase immobilized on a functional polymer modified glassy carbon electrode and its molecule recognition of glucose. *Polymers* **2019**, *11*, 115. [CrossRef]
25. Rowley-Neale, S.J.; Randviir, E.P.; Dena, A.S.A.; Banks, C.E. An overview of recent applications of reduced graphene oxide as a basis of electroanalytical sensing platforms. *Appl. Mater. Today* **2018**, *10*, 218–226.
26. Singh, D.; Shukla, V.; Khossossi, N.; Ainane, A.; Ahuja, R. Harnessing the unique properties of MXenes for advanced rechargeable batteries. *J. Phys. Energy* **2020**, *3*, 012005.
27. Hyun, K.; Han, S.W.; Koh, W.-G.; Kwon, Y. Direct electrochemistry of glucose oxidase immobilized on carbon nanotube for improving glucose sensing. *Int. J. Hydrogen Energy* **2015**, *40*, 2199–2206. [CrossRef]
28. da Silva, E.T.; Souto, D.E.; Barragan, J.T.; de F. Giarola, J.; de Moraes, A.C.; Kubota, L. Electrochemical biosensors in point-of-care devices: Recent advances and future trends. *ChemElectroChem* **2017**, *4*, 778–794. [CrossRef]

29. Ahmad, R.; Tripathy, N.; Park, J.-H.; Hahn, Y.-B. comprehensive biosensor integrated with a ZnO nanorod FET array for selective detection of glucose, cholesterol and urea. *Chem. Commun.* **2015**, *51*, 11968–11971.
30. Soto, D.; Orozco, J. Hybrid Nanobioengineered nanomaterial-based electrochemical biosensors. *Molecules* **2022**, *27*, 3841.
31. Ahmad, R.; Tripathy, N.; Hahn, Y. Highly stable urea sensor based on ZnO nanorods directly grown on Ag/glass electrodes. *Sens. Actuators B Chem.* **2014**, *194*, 290–295. [CrossRef]
32. Bauça, J.M.; Martínez-Morillo, E.; Diamandis, E. Peptidomics of urine and other biofluids for cancer diagnostics. *Clin. Chem.* **2014**, *60*, 1052–1061. [CrossRef]
33. Jiao, L.; Xu, W.; Wu, Y.; Wang, H.; Hu, L.; Gu, W.; Zhu, C. On the road from single-atom materials to highly sensitive electrochemical sensing and biosensing. *Anal. Chem.* **2023**, *95*, 433–443. [CrossRef]
34. Xu, J.; Wang, Y.; Hu, S. Nanocomposites of graphene and graphene oxides: Synthesis, molecular functionalization and application in electrochemical sensors and biosensors. A review. *Microchim. Acta* **2017**, *184*, 1–44.
35. Revuri, V.; Mondal, J.; Mohapatra, A.; Rajendrakumar, S.K.; Surwase, S.S.; Park, I.-K.; Park, J.; Lee, Y. Catalase-mimicking synthetic nano-enzymes can reduce lipopolysaccharide-induced reactive oxygen generation and promote rapid detection of hydrogen peroxide and l-cysteine. *J. Pharm. Investig.* **2022**, *52*, 749–764. [CrossRef]
36. Ayodhya, D. Recent progress on detection of bivalent, trivalent, and hexavalent toxic heavy metal ions in water using metallic nanoparticles: A review. *Results Chem.* **2023**, *5*, 100874. [CrossRef]
37. Silva, S.M.; Li, M.; Mendes, A.X.; Moulton, S. Reagentless protein-based electrochemical biosensors. *Analyst* **2023**, *148*, 1930–1938. [CrossRef] [PubMed]
38. Karimi-Maleh, H.; Liu, Y.; Li, Z.; Darabi, R.; Orooji, Y.; Karaman, C.; Karimi, F.; Baghayeri, M.; Rouhi, J.; Fu, L. Calf thymus ds-DNA intercalation with pendimethalin herbicide at the surface of ZIF-8/Co/rGO/C_3N_4/ds-DNA/SPCE; A bio-sensing approach for pendimethalin quantification confirmed by molecular docking study. *Chemosphere* **2023**, *332*, 138815. [CrossRef]
39. An, M.; Gao, Y. Proteomics and Bioinformatics. *Urin. Biomark. Brain Dis. Proteom. Bioinform.* **2015**, *13*, 345–354.
40. Kumar, R.R.; Kumar, A.; Chuang, C.-H.; Shaikh, M. Recent advances and emerging trends in cancer biomarker detection technologies. *Ind. Eng. Chem. Res.* **2023**, *62*, 5691–5713. [CrossRef]
41. Gopi, S.; Al-Mohaimeed, A.M.; Elshikh, M.S.; Yun, K. Facile fabrication of bifunctional SnO–NiO heteromixture for efficient electrocatalytic urea and water oxidation in urea-rich waste water. *Environ. Res.* **2021**, *201*, 111589. [CrossRef]
42. Nguyen, N.S.; Yoon, H. H, Nickel oxide-deposited cellulose/CNT composite electrode for non-enzymatic urea detection. *Sens. Actuators B Chem.* **2016**, *236*, 304–310. [CrossRef]
43. Sabir, A.S.; Pervaiz, E.; Khosa, R.; Sohail, U. An inclusive review and perspective on Cu-based materials for electrochemical water splitting. *RSC Adv.* **2023**, *13*, 4963–4993. [CrossRef] [PubMed]
44. Eskandarinezhad, S.; Wani, I.A.; Nourollahileilan, M.; Khosla, A.; Ahmad, T. Metal and metal oxide nanoparticles/nanocomposites as electrochemical biosensors for cancer detection. *J. Electrochem. Soc.* **2022**, *169*, 047504.
45. Chitare, Y.M.; Jadhav, S.B.; Pawaskar, P.N.; Magdum, V.V.; Gunjakar, J.L.; Lokhande, C.D. Metal oxide-based composites in nonenzymatic electrochemical glucose sensors. *Ind. Eng. Chem. Res.* **2021**, *60*, 18195–18217. [CrossRef]
46. Mohammed, M.-I.; Desmulliez, M.P. Lab-on-a-chip based immunosensor principles and technologies for the detection of cardiac biomarkers: A review. *Lab Chip* **2011**, *11*, 569–595. [CrossRef] [PubMed]
47. Hahn, Y.-B.; Ahmad, R.; Tripathy, N. Chemical and biological sensors based on metal oxide nanostructures. *Chem. Commun.* **2012**, *48*, 10369–10385. [CrossRef] [PubMed]
48. Agnihotri, A.S.; Varghese, A.; Nidhin, M. Transition metal oxides in electrochemical and bio sensing: A state-of-art review. *Appl. Surf. Sci. Adv.* **2021**, *4*, 100072. [CrossRef]
49. Padmanathan, N.; Sasikumar, R.; Thayanithi, V.; Razeeb, K. L-Alanine supported autogenous eruption combustion synthesis of Ni/NiO@RuO_2 heterostructure for electrochemical glucose and pH sensor. *ECS Sens. Plus* **2023**, *2*, 034601. [CrossRef]
50. Zheng, L.; Ma, S.; Wang, Z.; Shi, Y.; Zhang, Q.; Xu, X.; Chen, Q. Ni-P nanostructures on flexible paper for morphology effect of nonenzymatic electrocatalysis for urea. *Electrochim. Acta* **2019**, *320*, 134586. [CrossRef]
51. Tammam, R.H.; Saleh, M. On the electrocatalytic urea oxidation on nickel oxide nanoparticles modified glassy carbon electrode. *J. Electroanal. Chem.* **2017**, *794*, 189–196. [CrossRef]
52. Arul, P.; Gowthaman, N.; John, S.A.; Huang, S.-T. Urease-free Ni microwires-intercalated Co-ZIF electrocatalyst for rapid detection of urea in human fluid and milk samples in diverse electrolytes. *Mater. Chem. Front.* **2021**, *5*, 1942–1952. [CrossRef]
53. Lu, S.; Gu, Z.; Hummel, M.; Zhou, Y.; Wang, K.; Xu, B.B.; Wang, Y.; Li, Y.; Qi, X.; Liu, X. Nickel oxide immobilized on the carbonized eggshell membrane for electrochemical detection of urea. *J. Electrochem. Soc.* **2020**, *167*, 106509. [CrossRef]
54. Goda, M.A.; Abd El-Moghny, M.G.; El-Deab, M. Enhanced electrocatalytic oxidation of urea at CuOx-NiOx nanoparticle-based binary catalyst modified polyaniline/GC electrodes. *J. Electrochem. Soc.* **2020**, *167*, 064522. [CrossRef]
55. Amin, S.; Tahira, A.; Solangi, A.; Beni, V.; Morante, J.; Liu, X.; Falhman, M.; Mazzaro, R.; Ibupoto, Z.H.; Vomiero, A. practical non-enzymatic urea sensor based on NiCo2O4 nanoneedles. *RSC Adv.* **2019**, *9*, 14443–14451. [CrossRef]
56. Tomy, A.M.; Cyriac, J.M. Simultaneous detection of dopamine, uric acid and α-lipoic acid using nickel hydroxide nanosheets. *Microchem. J.* **2022**, *179*, 107550. [CrossRef]
57. Tyagi, M.; Tomar, M.; Gupta, V. Enhanced electron transfer properties of NiO thin film for the efficient detection of urea. *Mater. Sci. Eng. B* **2019**, *240*, 147–155. [CrossRef]

58. Arain, M.; Nafady, A.; Ibupoto, Z.H.; Sherazi, S.T.H.; Shaikh, T.; Khan, H.; Alsalme, A.; Niaz, A.; Willander, M. Simpler and highly sensitive enzyme-free sensing of urea via NiO nanostructures modified electrode. *RSC Adv.* **2016**, *6*, 39001–39006. [CrossRef]
59. Parsaee, Z. Synthesis of novel amperometric urea-sensor using hybrid synthesized NiO-NPs/GO modified GCE in aqueous solution of cetrimonium bromide. *Ultrason. Sonochem.* **2018**, *44*, 120–128. [CrossRef]
60. Irzalinda, A.; Gunlazuardi, J.; Wibowo, R. Development of a non-enzymatic urea sensor based on a Ni/Au electrode. *J. Phys. Conf. Ser.* **2020**, *1442*, 012054. [CrossRef]
61. Geim, A.K.; Novoselov, K.S. The rise of graphene. *Nat. Mater.* **2007**, *6*, 183–191. [CrossRef]
62. Durgalakshmi, D.; Rakkesh, R.A.; Mohanraj, J. Graphene–metal–organic framework-modified electrochemical sensors. In *Graphene-Based Electrochemical Sensors for Biomolecules*; Elsevier: Amsterdam, The Netherlands, 2019; pp. 275–296.
63. Tiwari, S.K.; Sahoo, S.; Wang, N.; Huczko, A. Graphene research and their outputs: Status and prospect. *J. Sci. Adv. Mater. Devices* **2020**, *5*, 10–29. [CrossRef]
64. Miao, J.; Fan, T. Flexible and stretchable transparent conductive graphene-based electrodes for emerging wearable electronics. *Carbon* **2023**, *202*, 495–527. [CrossRef]
65. Liu, B.-T.; Cai, X.-Q.; Luo, Y.-H.; Zhu, K.; Zhang, Q.-Y.; Hu, T.-T.; Sang, T.-T.; Zhang, C.-Y.; Zhang, D.-E. Facile synthesis of nickel@carbon nanorod composite for simultaneous electrochemical detection of dopamine and uric acid. *Microchem. J.* **2021**, *171*, 106823. [CrossRef]
66. Singh, A.; Sharma, A.; Arya, S. Deposition of Ni/RGO nanocomposite on conductive cotton fabric as non-enzymatic wearable electrode for electrochemical sensing of uric acid in sweat. *Diam. Relat. Mater.* **2022**, *130*, 109518. [CrossRef]
67. Naik, T.S.K.; Saravanan, S.; Saravana, K.S.; Pratiush, U.; Ramamurthy, P. A non-enzymatic urea sensor based on the nickel sulfide/graphene oxide modified glassy carbon electrode. *Mater. Chem. Phys.* **2020**, *245*, 122798. [CrossRef]
68. Nia, S.M.; Kheiri, F.; Jannatdoust, E.; Sirousazar, M.; Chianeh, V.A.; Kheiri, G.J. A highly sensitive non-enzymatic urea sensor based on $Ni(OH)_2/Mn_3O_4$/rGO/PANi nanocomposites using screen-printed electrodes. *J. Electrochem. Soc.* **2021**, *168*, 067504.
69. Qin, Y.; Chen, F.; Halder, A.; Zhang, M. Free-standing NiO nanosheets as non-enzymatic electrochemical sensors. *ChemistrySelect* **2020**, *5*, 2424–2429. [CrossRef]
70. Mohiuddin, A.K.; Yasmin, S.; Jeon, S. Co_xNi_{1-x} double hydroxide decorated graphene NPs for simultaneous determination of dopamine and uric acid. *Sens. Actuators A Phys.* **2023**, *355*, 114314. [CrossRef]
71. Muthusankar, E.; Ponnusamy, V.mK.; Ragupathy, D. Electrochemically sandwiched poly(diphenylamine)/phosphotungstic acid/graphene nanohybrid as highly sensitive and selective urea biosensor. *Synth. Met.* **2019**, *254*, 134–140. [CrossRef]
72. Foroughi, F.; Rahsepar, M.; Kim, H. A highly sensitive and selective biosensor based on nitrogen-doped graphene for non-enzymatic detection of uric acid and dopamine at biological pH value. *J. Electroanal. Chem.* **2018**, *827*, 34–41. [CrossRef]
73. Kumar, V.; Mahajan, R.; Kaur, I.; Kim, K. Simple and mediator-free urea sensing based on engineered nanodiamonds with polyaniline nanofibers synthesized in situ. *ACS Appl. Mater. Interfaces* **2017**, *9*, 16813–16823. [CrossRef] [PubMed]
74. Kumar, V.; Kaur, I.; Arora, S.; Mehla, R.; Vellingiri, K.; Kim, K. Graphene nanoplatelet/graphitized nanodiamond-based nanocomposite for mediator-free electrochemical sensing of urea. *Food Chem.* **2020**, *303*, 125375. [CrossRef]
75. Nguyen, N.S.; Das, G.; Yoon, H. H Nickel/cobalt oxide-decorated 3D graphene nanocomposite electrode for enhanced electrochemical detection of urea. *Biosens. Bioelectron.* **2016**, *77*, 372–377. [CrossRef]
76. Su, Y.; Hsu, W. Review field effect transistor biosensing: Devices and clinical applications. *ECS J. Solid State Sci. Technol.* **2018**, *7*, Q3196. [CrossRef]
77. Manimekala, T.; Sivasubramanian, R.; Dharmalingam, G. Nanomaterial-based biosensors using Field-Effect Transistors: A review. *J. Electron. Mater.* **2022**, *51*, 1950–1973. [CrossRef]
78. Kaisti, M. Detection principles of biological and chemical FET sensors. *Biosens. Bioelectron.* **2017**, *98*, 437–448. [CrossRef] [PubMed]
79. Pijanowska, D.G.; Torbicz, W. pH-ISFET based urea biosensor. *Sens. Actuators B Chem.* **1997**, *44*, 370–376. [CrossRef]
80. Rayanasukha, Y.; Pratontep, S.; Porntheeraphat, S.; Bunjongpru, W.; Nukeaw, J. Non-enzymatic urea sensor using molecularly imprinted polymers surface modified based-on ion-sensitive field effect transistor (ISFET). *Surf. Coat. Technol.* **2016**, *306*, 147–150. [CrossRef]
81. Silva, G.; Mulato, M. Urea detection using commercial field effect transistors. *ECS J. Solid State Sci. Technol.* **2018**, *7*, Q3014. [CrossRef]
82. Middya, S.; Bhattacharjee, M.; Bandyopadhyay, D. Reusable nano-BG-FET for point-of-care estimation of ammonia and urea in human urine. *Nanotechnology* **2019**, *30*, 145502. [CrossRef]
83. Sun, B.; Liu, Y.; Zhu, H.; Xing, L.; Bu, Q.; Ren, D. Recent advances of inkjet-printing technologies for flexible/wearable electronics. *Nanoscale* **2023**, *15*, 6025–6051.
84. Jagannathan, M.; Dhinasekaran, D.; Rajendran, A.R.; Subramaniam, B. Selective room temperature ammonia gas sensor using nanostructured ZnO/CuO@ graphene on paper substrate. *Sens. Actuators B Chem.* **2022**, *350*, 130833. [CrossRef]
85. Tonelli, D.; Gualandi, I.; Scavetta, E.; Mariani, F. Focus review on nanomaterial-based electrochemical sensing of glucose for health applications. *Nanomaterials* **2023**, *13*, 1883. [CrossRef]
86. Mohanraj, J.; Durgalakshmi, D.; Rakkesh, A. R Current trends in disposable graphene-based printed electrode for electrochemical biosensors. *J. Electrochem. Soc.* **2020**, *167*, 067523.
87. Barr, M.C.; Rowehl, J.A.; Lunt, R.R.; Xu, J.; Wang, A.; Boyce, C.M.; Im, S.G.; Bulović, V.; Gleason, K. Direct monolithic integration of organic photovoltaic circuits on unmodified paper. *Adv. Mater.* **2011**, *23*, 3500–3505. [CrossRef] [PubMed]

88. Hassan, R.Y.; Kamel, A.M.; Hashem, M.S.; Hassan, H.N.; Abd El-Ghaffar, M.A. A new disposable biosensor platform: Carbon nanotube/poly(o-toluidine) nanocomposite for direct biosensing of urea. *J. Solid State Electrochem.* **2018**, *22*, 1817–1823. [CrossRef]
89. Liu, Y.-L.; Liu, R.; Qin, Y.; Qiu, Q.-F.; Chen, Z.; Cheng, S.-B.; Huang, W.-H. Flexible electrochemical urea sensor based on surface molecularly imprinted nanotubes for detection of human sweat. *Anal. Chem.* **2018**, *90*, 13081–13087. [CrossRef]
90. Chou, J.-C.; Wu, C.-Y.; Kuo, P.-Y.; Lai, C.-H.; Nien, Y.-H.; Wu, Y.-X.; Lin, S.-H.; Liao, Y.-H. The flexible urea biosensor using magnetic nanoparticles. *IEEE Trans. Nanotechnol.* **2019**, *18*, 484–490. [CrossRef]
91. Berto, M.; Diacci, C.; Theuer, L.; Di Lauro, M.; Simon, D.T.; Berggren, M.; Biscarini, F.; Beni, V.; Bortolotti, C. Label free urea biosensor based on organic electrochemical transistors. *Flex. Print. Electron.* **2018**, *3*, 024001. [CrossRef]
92. Bao, Q.; Yang, Z.; Song, Y.; Fan, M.; Pan, P.; Liu, J.; Liao, Z.; Wei, J. Printed flexible bifunctional electrochemical urea-pH sensor based on multiwalled carbon nanotube/polyaniline electronic ink. *J. Mater. Sci. Mater. Electron.* **2019**, *30*, 1751–1759. [CrossRef]
93. Randviir, E.P.; Banks, C. A review of electrochemical impedance spectroscopy for bioanalytical sensors. *Anal. Methods* **2022**, *14*, 4602–4624. [CrossRef]
94. Robinson, C.; Juska, V.B.; O'Riordan, A. Surface chemistry applications and development of immunosensors using electrochemical impedance spectroscopy: A comprehensive review. *Environ. Res.* **2023**, *237*, 116877. [CrossRef] [PubMed]
95. Balasubramani, V.; Chandraleka, S.; Rao, T.S.; Sasikumar, R.; Kuppusamy, M.; Sridhar, T. Recent advances in electrochemical impedance spectroscopy based toxic gas sensors using semiconducting metal oxides. *J. Electrochem. Soc.* **2020**, *167*, 037572. [CrossRef]
96. Ameer, S.; Ibrahim, H.; Yaseen, M.U.; Kulsoom, F.; Cinti, S.; Sher, M. Electrochemical impedance spectroscopy-based sensing of biofilms: A comprehensive review. *Biosensors* **2023**, *13*, 777. [CrossRef]
97. Meddings, N.; Heinrich, M.; Overney, F.; Lee, J.-S.; Ruiz, V.; Napolitano, E.; Seitz, S.; Hinds, G.; Raccichini, R.; Gaberšček, M. Application of electrochemical impedance spectroscopy to commercial Li-ion cells: A review. *J. Power Sources* **2020**, *480*, 228742. [CrossRef]
98. Salarizadeh, N.; Habibi-Rezaei, M.; Zargar, S. NiO–MoO_3 nanocomposite: A sensitive non-enzymatic sensor for glucose and urea monitoring. *Mater. Chem. Phys.* **2022**, *281*, 125870. [CrossRef]
99. Shekh, M.I.; Amirian, J.; Du, B.; Kumar, A.; Sharma, G.; Stadler, F.J.; Song, J.C. Electrospun ferric ceria nanofibers blended with MWCNTs for high-performance electrochemical detection of uric acid. *Ceram. Int.* **2020**, *46*, 9050–9064. [CrossRef]
100. Albaqami, M.D.; Medany, S.S.; Nafady, A.; Ibupoto, M.H.; Willander, M.; Tahira, A.; Aftab, U.; Vigolo, B.; Ibupoto, Z. The fast nucleation/growth of Co_3O_4 nanowires on cotton silk: The facile development of a potentiometric uric acid biosensor. *RSC Adv.* **2022**, *12*, 18321–18332. [CrossRef] [PubMed]